Nucleic Acids Research, 1993, Vol. 21, No. 1 99–103

Atomic force microscopy of oriented linear DNA molecules labeled with 5nm gold spheres

Wen-Ling Shaiu, Drena D.Larson, James Vesenka and Eric Henderson*
Department of Zoology and Genetics, Iowa State University, Ames, IA 50011, USA

Received September 24, 1992; Revised and Accepted November 25, 1992

ABSTRACT

The atomic force microscope (AFM;1) can image DNA and RNA in air and under solutions at resolution comparable to that obtained by electron microscopy (EM) (2–7). We have developed a method for depositing and imaging linear DNA molecules to which 5nm gold spheres have been attached. The gold spheres facilitate orientation of the DNA molecules on the mica surface to which they are adsorbed and are potentially useful as internal height standards and as high resolution gene or sequence specific tags. We show that by modulating their adhesion to the mica surface, the gold spheres can be moved with some degree of control with the scanning tip.

INTRODUCTION

The atomic force microscope (1) is capable of generating high, sometimes atomic, resolution images of biological and non-biological surfaces (8, 9). DNA has been one of the most widely utilized test substances for imaging of biological samples by AFM (2–7, 10, 11). Several of these studies have shown that it is possible to immobilize and image DNA in air and under solutions at resolution comparable to that obtained by electron microscopy. Individual DNA molecules have been severed by the AFM at desired positions and small fragments removed (2, 5, 11). The ability of the AFM to image and dissect small pieces of DNA portends its utility as an instrument for gene isolation and manipulation.

We have begun to develop techniques for localization of specific sequences and directed recovery and manipulation of DNA fragments by AFM. Our approach has been to incorporate biotinylated nucleotides into DNA and subsequently react the biotinylated DNA molecules with a streptavidin-gold (SAG) conjugate, in this case 5nm diameter gold spheres. We show that DNA labeled with gold spheres can be deposited in an oriented fashion and reliably imaged by AFM. In addition, we demonstrate that the gold spheres can be moved easily, suggesting that they could be used as physical handles for manipulating attached DNA. Current work is focused on exploiting the properties of gold spheres to visualize specific genes in chromatin and to isolate the tagged DNA fragments.

MATERIALS AND METHODS

DNA labeling

Plasmid DNA, pUC119, was prepared by alkaline lysis and CsCl-EtBr gradient purification (12). DNA was 5′ end-labeled with bio-dUTP (Enzo Biochem, NY) by using Klenow fragment of *E.coli* DNA polymerase I to fill in 5′ overhanging ends generated by digestion with Hind III. Unincorporated bio-dUTP was removed by ethanol precipitation, and the bio-dUTP labeled DNA was resuspended in 10mM Tris–HCl (pH 7.2), 5mM MgOAc, 50mM NH_4OAc, 1mM EDTA (TMNE) and incubated with 1 μl streptavidin-gold conjugate (Amersham) for 60 minutes at 25°C. The DNA-bound gold particles were separated from unbound gold conjugate by chromatography through Bio-gel A-50 (Biorad) in 20mM Tris–HCl (pH 7.5), 100mM NaOAc (TN). Fractions containing DNA were pooled and ethanol precipitated.

Sample deposition and AFM imaging

Biotin-streptavidin-gold-DNA (BSG-DNA) in 20mM Tris–HCl (pH 7.2), 100mM NaOAc and 5mM $MgCl_2$ (TNM) (W. Rees, personal communication) was deposited directly onto freshly cleaved mica (Ted Pella, Inc.) for imaging in the AFM, or further concentrated by ethanol precipitation. The BSG-DNA was allowed to adsorb for 5 minutes (much shorter times worked equally well and in some experiments only a few seconds adsorption was required). The mica was rinsed with 1 ml ddH_2O or dragged across a 10mM NH_4OAc solution ten times and immediately and exhaustively dried with N_2 gas with the gas flow orthogonal to the surface. DNA prepared in this way was imaged either under propanol or in air at relative humidity $< 10\%$ (2–7, 10, 11, 13, 14). For this report, all images were collected on a Nanoscope II or Nanoscope III (Digital Instruments, Inc., Santa Barbara, CA) using Si_3N_4 tips (Digital Instruments, Inc., Santa Barbara, CA). In height mode images, the gray scale represents the sample height with lighter features being taller. In error signal mode (15) images, the error signal is displayed, rather than the true image height. All height measurements were made on height mode images.

Data preparation

For data presentation, image files were imported into the Macintosh program Image 1.43 (custom settings: 400×400 or 512×512, 2048 header, 16 bit signed, swap bites, calibrate off)

* To whom correspondence should be addressed

and converted to PICT format for preparation of figures in Aldus Freehand 3.1. Statistical analysis of height and length measurements was carried out on Kaleidagraph graphics program (Synergy Software, Reading, PA).

RESULTS

Images of unlabeled double-stranded DNA molecules in dry air (3, 10, 11, 13, 14) or under propanol (2, 4, 10) were routinely collected (Fig. 1). The widths of DNA were narrower in propanol than air, similar to results reported elsewhere (2, 4, 10). Since the two methods provided approximately equivalent lengths and heights under our conditions, and the air preparation is simpler, all measurements reported in this study were made on images collected in dry air.

Figure 2 shows the general procedure used for end-labeling DNA with bio-dUTP and SAG (see Materials and Methods for details). To obtain sharp images with a low background (i.e., with very little unbound SAG and/or salt deposits), the indicated purification steps were essential. Unlike EM, in which many contaminants are transparent to the electron beam, small contaminants such as salt deposits can obscure images of DNA molecules obtained by AFM. Therefore, after removal of unbound SAG by column chromatography, the DNA sample was further desalted by ethanol precipitation, deposited onto the mica from low or volatile salt solutions and rinsed after deposition with the same salt solutions or distilled water. The overall efficiency of labeling was approximately 60% under the conditions described in Materials and Methods. A number of molecules were observed with the appearance of a protein (i.e., streptavidin) attached to an end, but no gold sphere (data not shown). Detachment of streptavidin from SAG has been frequently observed by EM (E.Henderson, unpublished observation).

End-labeled DNA preparations appeared as single or multiple strands with gold spheres at one or both ends, as expected (Fig. 3). Although most SAG-containing molecules were terminally labeled (~70%), some molecules had SAG attached within the DNA strand. This is most likely due to incorporation of bio-dUTP at nicks, since the plasmid DNA preparation contained ~30% nicked circular DNA prior to restriction enzyme digestion (data not shown).

Strikingly, the gold labeled molecules in a given field were often oriented in the same general direction. This suggests that the gold particle adhered first to the mica substrate during the drying process (with N_2 gas) and that the DNA flowed in the direction of the N_2 gas before it absorbed to the surface. In other words, the DNA was immobilized by the gold sphere at one end and extended in a direction determined by liquid and N_2 gas flow. Molecules apparently lacking gold at an end (although possibly having bound streptavidin) also showed preferred orientation in some cases. Thus, the DNA may align to some extent in the N_2 stream even in the absence of a gold end label. However, unlabeled molecules with an apparently random orientation were common, whereas non-aligned gold labeled molecules were infrequently seen.

The apparent contour lengths of 121 DNA molecules were measured (Fig. 4; see Materials and Methods). These molecules had an average length of 889 ± 91nm. The predicted value for the plasmid used is 1074nm in the B-form and 804 in the A-form (16). Since these molecules were imaged under very dry conditions (<10% relative humidity), the correspondence between the measured contour length and that expected for A-

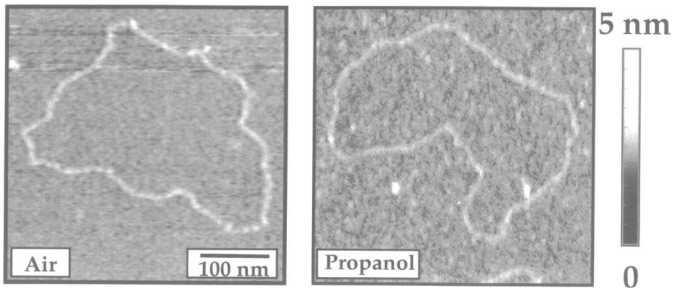

Figure 1. Typical height mode (see Materials and Methods) images of plasmid DNA molecules collected under propanol and in dry air (relative humidity ~10%). In these gray scale images tall features are lighter and flat features are darker. The gray scale bar on the right indicates the gray level spectrum and corresponding feature heights.

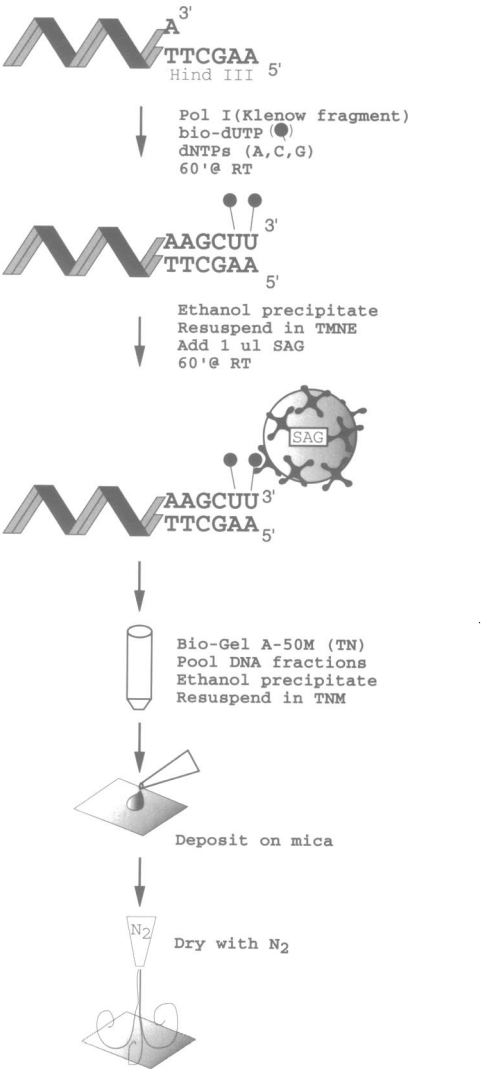

Figure 2. Diagram of the procedures used for labeling, purification and deposition of DNA samples for AFM imaging. Details and buffer abbreviations are in Materials and Methods.

form (dehydrated) DNA may reflect a conformational property of the DNA helix.

The average height of the DNA was 0.54 ± 0.12nm (n=68, Fig. 4). The expected height of duplex DNA is approximately 2.0nm. The 4-fold discrepancy between the measured height and the expected height is not due to inaccuracy in the calibration of the Z-piezo since it was calibrated using atomic steps of highly oriented pyrolytic graphite and was within 20% of the expected value (2.6 Å) in all cases. Two possible explanations include sample compression due to pressure from the scanning tip (3) and embedding of the DNA in residual buffer salts (J.Vesenka, unpublished).

The height of the SAG measured by AFM was 5.8 ± 1.5nm (n=108, Fig. 4). This heterogeneity precludes use of currently commercially available SAG as an internal height standard (see Discussion). Determination of true sample width from measured values requires detailed knowledge about the tip shape (3, 11, 17). Since this information is lacking, width measurements are not presented.

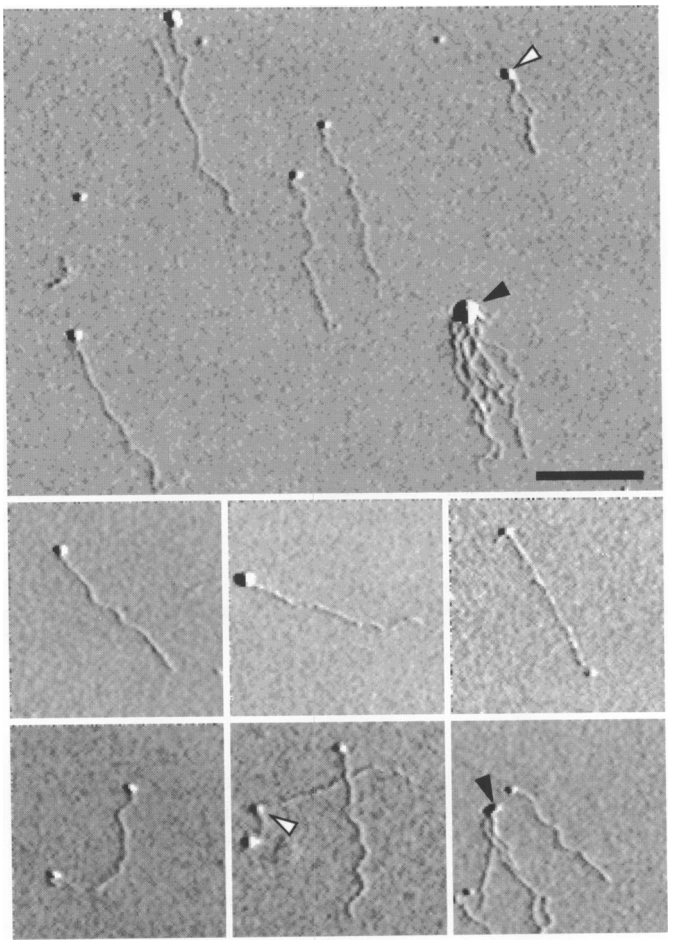

Figure 3. Typical field and gallery of individual end labeled DNA molecules. The labeled DNA molecules are oriented in the same general direction as a consequence of the drying procedure. White arrowheads indicate molecules with internal labels. The internal labeling results from nick translation of nicked circular plasmid DNA during the end labeling procedure. Black arrowhead indicates a multimeric structure commonly observed, presumably resulting from biotin/streptavidin network formation. Images were taken in error signal mode (see Materials and Methods). Bar = 500nm.

Height measurements were dependent on the scan direction. This dependence is a consequence of bending of the AFM cantilever due to strong interaction between the tip and the sample (or hydration layers on both) and is discussed in detail elsewhere (13, 14, 18, 19). For the height measurements reported here, the scan angle was optimized by piezo rotation at each area imaged to give overlapping oscilloscope tracings in both scan directions. The scan angle was frequently between 70° and 120°. This rotation often gives the most accurate height measurements (19, J.Vesenka, unpublished.)

It was possible to move the SAG spheres with the scanning tip by altering the humidity of the imaging environment. Similar results have been obtained with unconjugated gold spheres (J.Vesenka, unpublished). Figure 5 shows two examples of this process. The quality of the DNA image decayed as the humidity was increased as reported previously (3, 11, 13, 14). Concomitant with this decay was an increase in the imaging force, presumably due to increased meniscus forces between the tip and the sample. In the first series (Fig 5A), the force was not adjusted to compensate for the increase in humidity and the DNA became severed in several places at higher humidities. Movement of the SAG is indicated by diagonal lines in the scan taken at highest

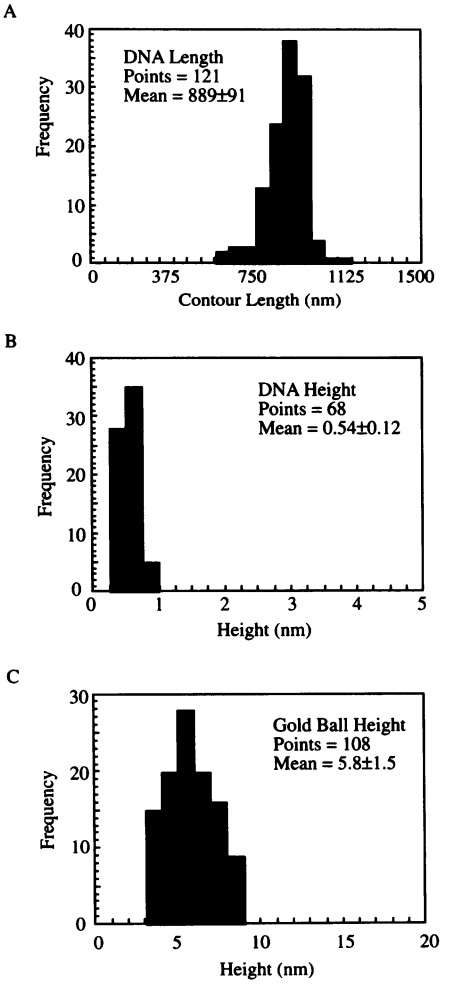

Figure 4. Histogram showing the contour length distribution for the DNA and the height distributions for the DNA and SAG used in this study.

humidity (~60% relative humidity). When the humidity was subsequently reduced, the area previously scanned was visible, with the DNA apparently highly fragmented and gold accumulation at the edges of the field. In the second series (Fig. 5B), the applied vertical force was monitored constantly and maintained at the initial level (10–20 nN). Again the gold was released from the surface at ~60% relative humidity and the DNA was fragmented. These results demonstrate that changes in humidity can be exploited to manipulate colloidal gold spheres and DNA, but that methods to avoid concomitant damage to DNA samples must be established.

DISCUSSION

We have developed a method for imaging gold-labeled DNA molecules by AFM. Gold spheres 5nm in diameter are attached to DNA molecules through a biotin-streptavidin linkage. In addition to permitting localization of regions of the DNA into which the biotinylated nucleotide has been incorporated, this method allows the oriented deposition of linear DNA molecules. Since the AFM and related microscopes have atomic resolution on hard surfaces, it has been suggested that they have considerable potential for use in direct DNA sequencing (20). Methods for deposition of linear DNA fragments in an oriented and elongated fashion, such as that described here, would facilitate this effort. In the near term, since the method presented here is simple and rapid, it may be possible to develop techniques in which direct visualization of DNA samples with the AFM would compliment or replace analytical gel electrophoretic methods (e.g., for restriction mapping) or electron microscopy methods (e.g., for mapping DNA replication origins). Accurate mapping of DNA locations by AFM requires that contour length measurements be precise. In this study, images were collected under conditions expected to facilitate the formation of A-form DNA. Under these conditions we found that the average contour length for the molecules measured was within 11% of the expected contour length for A-form DNA based on an average axial rise of 2.56Å/bp (16). Therefore, these results suggest that the AFM has the potential for use in mapping experiments within 11% error. This value can easily be improved by, for example, higher pixel density and more sophisticated contour length measuring systems. Moreover, it is possible that the average value used to calculate the expected A-form contour length for the plasmid used in this study may be misleading since it does not account for sequence specific variation in the axial rise value.

Since the AFM can be used to dissect as well as image DNA, physical handles such as gold spheres may be useful for manipulation and recovery of DNA fragments generated by AFM scission. In this study, the SAG was manipulated readily with the scanning tip but only at the cost of fragmenting the attached DNA. Future efforts will focus on devising methods for recovering specific DNA molecules in intact form. Development of techniques for imaging and manipulating DNA under aqueous conditions will greatly facilitate this effort.

The use of 5nm gold spheres as tags could, in principle, provide a convenient size calibration standard. This type of non-compressible standard (J.Vesenka, unpublished) would be extremely useful in assessing the degree of compression of samples by the scanning tip. If the measured height of the gold spheres is not accurate due to piezo calibration error one could still calculate the true height of the sample (in its compressed form) by a simple scaling procedure using the known gold sphere diameter determined by another method (e.g., EM). To serve as a reliable scaling standard, however, the gold spheres must be homogeneous in size, a requirement clearly not met by the SAG used in this study. Commercially available unconjugated gold spheres that are much more homogeneous in size than the SAG used here function well at size standards when mixed with biological samples (J.Vesenka, unpublished). Since attachment of gold spheres to the sample is not required if they are to serve as height standards only, their use should dramatically improve the accuracy of the height measurements in the AFM.

Methods for single molecule manipulation and imaging by AFM are rapidly evolving. Based on the demonstrated capabilities of the AFM it is likely to become a powerful tool for gene manipulation and physical mapping, a major near term goal of the Human Genome Project.

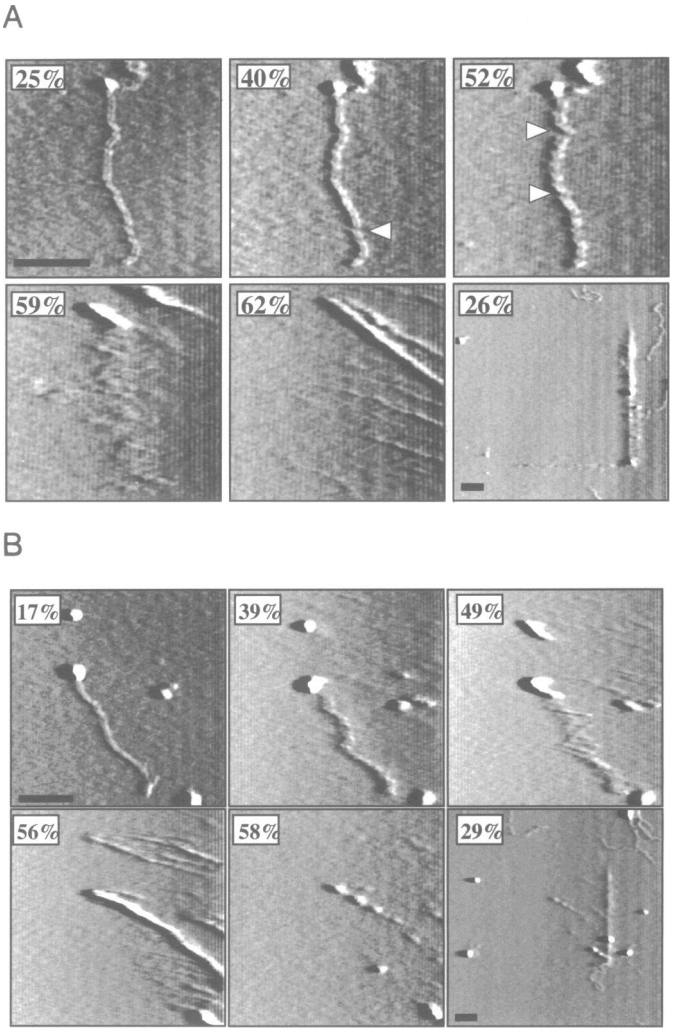

Figure 5. Humidity regulated movement of gold spheres by the AFM scanning tip. **(A)** The applied vertical force increased to greater than 120 nN as the humidity increased, resulting in DNA damage prior to release from the substrate (white arrowheads). **(B)** The applied vertical force was maintained between 10–20 nN. DNA damage was still evident in this experiment. In both cases, the last frame shows a larger field scan of the area shown in the preceding frames (made after reducing the humidity to < 26%). The gold spheres have accumulated at one edge. Relative humidity is indicated in the corner of each frame. Images were taken in error signal mode. Bar = 250nm.

ACKNOWLEDGMENTS

The authors are grateful to Daniel Jondle for help with height measurements, and to the reviewers for helpful comments and criticisms. This work was supported by NSF grant DIR-9004649 (EH), NIH grants GM41023 (EH) and GM41899 (DDL) and Iowa State University (EH and DDL). Journal Paper No. J-15095 of the Iowa Agriculture and Home Economics Experiment Station, Ames, Iowa. Project No. 3064.

REFERENCES

1. Binnig, G., Quate, C. F. and Gerber, C. (1986) Phys. Rev. Lett. **56**, 930–933.
2. Hansma, H., Vesenka, J., Siegerist, C., Kelderman, G., Morret, H., Sinsheimer, R. L., Elings, V., Bustamante, C. and Hansma, P. K. (1992) Science. **256**, 1180–1184.
3. Bustamante, C., Vesenka, J., Tang, C. L., Rees, W., Guthold, M. and Keller, R. (1991) Biochemistry. **31**, 22–26.
4. Hansma, H., Sinsheimer, R. L., Li, M.-Q. and Hansma, P. K. (1992) Nuc. Acids. Res. **20**, 3585–3590.
5. Henderson, E. (1992) Nuc. Acids Res. **20**, 445–447.
6. Henderson, E. (1992) J. Micros. **167**, 77–84.
7. Yang, J., Takeyasu, K. and Shao, Z. (1992) FEBS Letters. **301**, 173–176.
8. Drake, B., Prater, C. B., Weisenhorn, A. L., Gould, S. A., Albrecht, T. R., Quate, C. F., Cannell, D. S., Hansma, H. G. and Hansma, P. K. (1989) Science. **243**, 1586–1589.
9. Hoh, J. H. and Hansma, P. K. (1992) Trends in Cell Biology. **2**, 208–213.
10. Vesenka, J., Hansma, H., Siegerist, C., Siligardi, G., Schabtach, E. and Bustamante, C. (1992) Scanning force microscopy of circular DNA and chromatin in air and propanol. SPIE Conf. Proc. **1639**, 127–137.
11. Vesenka, J., Guthold, M., Tang, C. L., Keller, D., Delaine, C. and Bustamante, C. (1992) Ultramicroscopy. **42–44**, 1243–1249.
12. Sambrook, J., Fritsch, E.F. and Maniatis T. (1989) Molecular Cloning: A Laboratory Manual. Cold Spring Harbor Laboratory Press, Cold Spring Harbor.
13. Thundat, T., Warmack, R. J., Allison, D. P., Bottomley, L. A., Lourenco, A. J. and Ferrell, T. L. (1992) J. Vac. Sci. Tech. A. **10**, 632–635.
14. Thundat, T., Allison, D. P., Warmack, R. J. and Ferrell, T. L. (1992) Ultramicroscopy. **42–44**, 1101–1106.
15. Putman, C. A. J., van der Werk, K., de Grooth, B. G., van Hulst, N. F., Greve, J. and Hansma, P. K. (1992) SPIE. **1639**, 198–204.
16. Saenger, W. Principles of Nucleic Acid Structure. (1988) Springer-Verlag Inc., New York.
17. Keller, D., Deputy, D., Alduino, A. and Luo, K. (1992) Ultramicroscopy. **42–44**, 1481–1489.
18. Zenhausern, F., Adrian, M., ten Heggeler-Bordier, B., Eng, L.M. and Descouts, P. (1992) Scanning. **14**, 212–217.
19. Radmacher, M., Tillmann, R.W., Fritz, M. and Gaub, H.E. (1992) Science. **257**, 1900–1905.
20. Hansma, H. G., Weisenhorn, A. L., Gould, S. A. C., Sinsheimer, R. L., Gaub, H. E., Stucky, G. D., Zaremba, C. M. and Hansma, P. K. (1991) J.Vac. Sci. Tech. B. **9**, 1282–1284.